A Modified Model Reference Adaptive Control for High-Performance Pantograph Robot Mechanism

[1]LAYLA M. EL-TEHEWY, [2]MOHAMED A. SHAMSELDIN, [3]MOHAMED SALLAM,
[4]A. M. ABDEL GHANY

Department of Mechatronics Engineering, MTI University, Cairo, EGYPT.[1]
Department of Mechanical Engineering, Future University in Egypt, Cairo, EGYPT.[2]
Department of Mechanical Engineering, Egyptian-Chinese University (on leave from Helwan University, Cairo, EGYPT.[3]
Department of Control Engineering, Higher Engineering Institute, Thebes Academy, (on leave from Helwan University), Cairo, EGYPT.[4]

Abstract: - Pantograph Robot Mechanism is considered a type of parallel manipulator which has been developed largely for industrial applications that need high accuracy and speed. Whereas, it needs a high- performance controller to track preselected trajectory planning. It is also able to carry higher weights than the open-chain mechanism with suitable accuracy and stability; this is because it consists of four active links and one passive link, instead of two links as in the open chain. This study presents a mathematical model for a closed chain pantograph mechanism, where the boundary conditions are taken into account. A complete MATLAB Simulink has been developed to simulate the dynamics of the pantograph robot mechanism. To validate the proposed mathematical model of the pantograph, the corresponding Simscape model had been developed. Also, three different tracking controllers were designed. The first control is the PID controller which had optimized by Flower Pollination (FP) optimization. The second control is an enhanced Nonlinear PID (NLPID) controller where its parameters were obtained by Flower Pollination (FP) optimization based on the effective objective function. The third control is the model reference adaptive control. A comparative study between the control techniques was accomplished. A rectangular trajectory was selected to be a position reference of the end effector of the pantograph robot. This task was done using the proposed controllers to investigate the performance. The results show that the model reference adaptive control has a better performance compared to the NLPID and PID controllers. The end effector has a less rise time and settling time with high accuracy in the case of the model reference adaptive control.

Key-Words: - Flower Pollination; Pantograph Robot; Nonlinear PID (PID); Adaptive PID control; Manipulator Dynamics; model reference adaptive control (MRAC).

Received: April 15, 2021. Revised: September 9, 2021. Accepted: October 1, 2021. Published: October 8, 2021.

1 Introduction

Parallel robots have become a necessary part of the robots used in academia and industry [1]. Besides, with the rapid development of parallel robots, the research on mechanism theory, mobility analysis, dimensional synthesis, kinematics and dynamics modeling, and design optimization has been increasing on a large scale [2]. The development of parallel robotics and controllable mechanism has become widely used as a mechanical design, as shown in Fig. 1 [3].

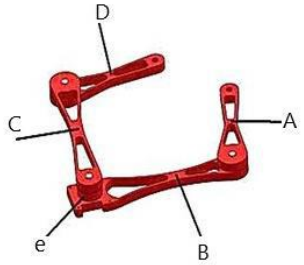

Fig. 1. Five Bar Planar (Pantograph).

The name pantograph refers to the five-sided links used. Four of the five links are moving platforms and the fifth one is the base platform [4]. The five-bar planar manipulator is a relatively simple mechanism that has two-degree-of-freedom (DOF) and its kinematics is explicit [5]. However, its characteristics are high speed, high accuracy, low inertia, and carrying more weights [6].

For these reasons, it draws a lot of researchers' attention. Some prototypes and commercial products were made, such as the 'double SCARA' RP-AH series offered by Mitsubishi Electrics, and DexTAR, a five-bar planar manipulator designed by ETS. The five-links planar of the pantograph, which is a simple two degree of freedom (DOF) mechanism (Fig. 2), one of them (L0) is passive and the other four links (L1, L2, L3, L4) are active.

The system contains only five revolute joints (Fig. 2). Links 1 and 4 are the driving links. With the help of the appropriate rotation of the actuating links, the characteristic point e of the system can follow the desired planar trajectory in the region of the working zone [7].

Especially, the need for exactly adaptive automation in varied applications has led to higher requirements for operational accuracy and cycle time with robots [8]. Examples of such needs are higher precision assembly, faster product handling, surface finishing, better measurements, surface finishing, and milling capabilities [9]. Additionally, there is a high demand for off-line programming to eliminate touch-up of programmed positions; in other words, robots must perform their task with better load capacity and accuracy in operations. A general trend of meeting these requirements is to make use of parallel robots, which have excellent potential capabilities, including high rigidity, high accuracy, and high loading capacities [10].

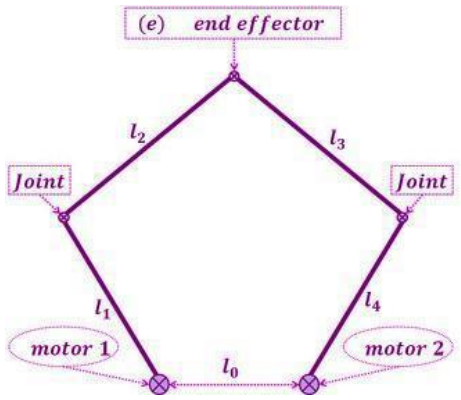

Fig. 2. Two-DOF Mechanism.

The PID controller is linear and commonly used in engineering applications because of its simple scheme and satisfying performance. Its gains are adjusted to assure both stability and performance. For such purpose, several design techniques were suggested in particular, intelligent techniques (Genetic Algorithm (GA), Evolutionary Programming (EP), and Simulated Annealing (SA), etc..) and animal mimics (Bacterial Foraging Algorithm (BFA), Bee's Algorithm (BA), Particle Swarm Optimization (PSO), etc...) were studied [4],[5],[6]. Another category of PID controllers is the Nonlinear PID (NLPID) that can be improved the dynamic response of the conventional PID controller [11]. The NLPID controller has the advantage of adaptive, self-learning, online adjustment, and relatively lower requirements for stability and precision of controlled objects. Moreover, the structure of the NLPID controller is simple and reliable [12].

In the first step, the initial values of NLPID control parameters can be estimated by try and error and this takes a long time for the simulation. In the second step, the tuning optimization techniques used usually rely on the computation of an objective function representing the desired performance while satisfying the system constraints [13]. So, the Flower Pollination (FP) based on an effective objective function will be used to find the optimal values of controller parameters [14].

Adaptive control is one of the extensively used control strategies to design advanced control systems for better performance and accuracy. Model reference adaptive control (MRAC) is a direct adaptive strategy with some adjustable controller parameters and an adjusting mechanism to adjust them [15]. As compared to the well-known and simple structured fixed gain PID controllers, adaptive controllers are very effective to handle the parameters uncertainty and environmental fluctuations [16]. See also the interesting [17] and [18].

In this paper three advanced control strategy have been adopted and compared. The first control technique is Optimal PID controller based on Flower Pollination optimzation technique which shows unsatisfied performance. The second technique is an enhanced nonlinear PID (NLPID) controller that presents a acceptable solution for system nonlinearity. The third technique is established on MRAC. Implementing MRAC shows a reasonable performance but it has high overshooting and continuous steady state error. Combining MRAC with PID control compensator will eliminate both the overshoots and steady state error.

2 PANTOGRAPH MECHANISM MODEL:

2.1 Direct Kinematics

The constrain of the five-link mechanisms as shown in Fig. 3 is given by

$$L_1\bar{a}_1+L_2\bar{b}_1-L_3\bar{c}_1-L_4\bar{d}_1-L_5\bar{n}_1=0 \quad (1)$$

Where L_i for i=1,…..,5 is the length of links, $(\bar{a}_1, \bar{b}_1, \bar{c}_1, \bar{d}_1, \bar{n}_1)$ are unit vectors [7] . The relation between the task space $(X=(x_e \ y_e)^T)$ and joint space $(\theta=(\theta_1 \ \theta_2 \ \theta_3 \ \theta_4)^T$ of the five-link mechanism system can be calculated, where x and y are the Cartesian coordinates of Joint e with respect to the plane (n_1 , n_2) [13], as shown in Fig. 3.

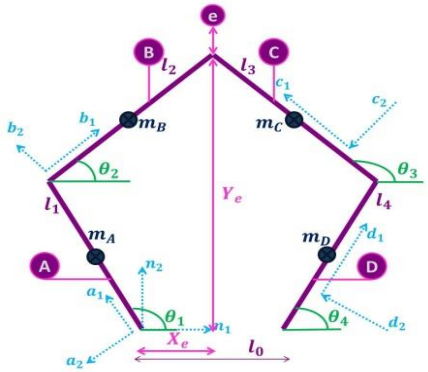

Fig. 3. Direct Kinematics Mechanism.

The equations of x and y using θ1 and θ4 are de-fined as following [14]:

$$x_e=L_1\cos\theta_1+L_2\cos\theta_2=L_3\cos\theta_3+L_4\cos\theta_4+I \quad (2)$$

$$y_e = L_1 \sin\theta_1 + L_2 \sin\theta_2 = L_3 \sin\theta_3 + L_4 \sin\theta_4 \quad (3)$$

Equations (2) and (3) can simulate the forward kinematics of the five-link mechanism. From equations (1, 2, and 3) θ_2 can be expressed in terms of θ_1 and θ_4 by the holonomic constraints. Where θ_2 is dependent angle and has to be described using the active angle of the device (θ_1 and θ_4).

Newton-Raphson method or Trigonometry method can be used to find θ_3 and θ_2 . In this work, the trigonometry method was used as follows:

$$\theta_3 = 2\tan^{-1}\left(\frac{A \pm \sqrt{A^2+B^2-C^2}}{B-C}\right) \quad (4)$$

Where,

$$A = 2L_3 L_4 \sin\theta_4 - 2L_1 L_3 \cos\theta_1$$

$$B = 2L_3L_5 - 2L_1L_3\cos\theta_1 + 2L_4L_3\cos\theta_4$$

$$C = L_1^2 - L_2^2 + L_3^2 + L_4^2 + L_5^2 - L_1L_4\sin\theta_1\sin\theta_4 - 2L_1L_5\cos\theta_1 - 2L_4L_5\cos\theta_4\cos\theta_1$$

And,

$$\theta_2 = \sin^{-1}\left(\frac{L_3\sin\theta_3 + L_4\sin\theta_4 - L_1\sin\theta_1}{L_2}\right) \quad (5)$$

. 2.2 Inverse Kinematics

The direct relation between the coordinates of the end-effector and link lengths to the actuating anglesθ_1 and θ_4 is in the following equations [17]:

$$\theta_1 = 2\tan^{-1}\left(\frac{-E \pm \sqrt{D^2+E^2-F^2}}{-D-F}\right) \quad (6)$$

Where,

$$D = x_e$$
$$E = y_e$$
$$F = \frac{L_1^2 - L_2^2 + x_e^2 + y_e^2}{2L_1}$$

And

$$\theta_4 = 2\tan^{-1}\left(\frac{-H \pm \sqrt{G^2+H^2-I^2}}{-G-I}\right) \quad (7)$$

Where,

$$G = x_e - L_5$$
$$H = y_e$$

$$I = \frac{L_4^2 + L_5^2 - L_3^2 - 2x_cL_5 + x_e^2 + y_e^2}{2L_4}$$

The link lengths are constant for the robot, which helps to easily solve the above equations. From equations (12) and (13) it can be obtained θ_1 and θ_4 without known θ_2 and θ_3 [14]. The only inputs needed for controlling the five-link mechanism are the location of the end-effector (x_e and y_e).

2.3 Boundary Conditions

It is an important part which is the permissible boundary for a mechanism so that the link does not reach the singularity state during the path [18]. For this to be achieved Q_5 must not be equal to 180 degrees but rather greater.

So, $Q_5 < 180$ shown in Fig. 4

$$Q_5 = 540 - (180+\theta_1) - (180-\theta_4+\theta_3) - (180+\theta_1-\theta_2) - (\theta_4) \quad (8)$$

So the first boundary is:

$$Q_5 = (\theta_2 - \theta_3) < 180 \quad (9)$$

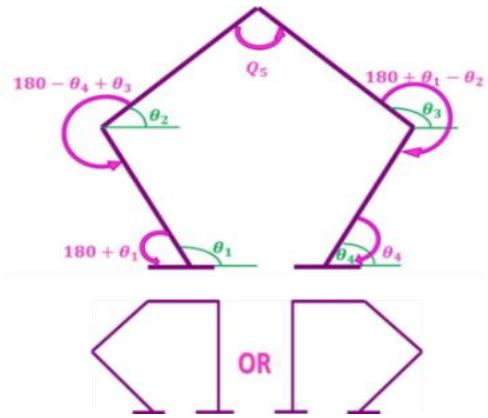

Fig. 4. Direct Kinematics Mechanism.

Second one: In order for the mechanism not to reach the position shown in Fig. 4, θ_2 must be greater than θ_1.

Third one: θ_4 must be greater than θ_3.

$$(\theta_2 > \theta_1) \quad (10)$$

$$(\theta_4 > \theta_3) \quad (11)$$

The three rules (9), (10), and (11), can be implemented using the logic gate (AND).

2.4 Equation of Motion

Lagrangian equation:

$$T = \text{Torque} = \frac{\partial}{\partial t}\frac{\partial L}{\partial \dot{\theta}_i} - \frac{\partial L}{\partial \theta_i} \quad (12)$$

By using Lagrangian equation obtain by torque, T1 and T2, Where (A, B, C, D, E, F) are constants.

$$T_1=\left(A_1\ddot{\theta}_1+B_1\ddot{\theta}_4+C_1\dot{\theta}_1+D_1\dot{\theta}_4\right) - \left(E_1\dot{\theta}_1{}^2+F_1\dot{\theta}_4{}^2+G_1\dot{\theta}_1\dot{\theta}_4\right) \quad (13)$$

$$T_2=\left(A_2\ddot{\theta}_1+B_2\ddot{\theta}_4+C_2\dot{\theta}_1+D_2\dot{\theta}_4\right) - \left(E_2\dot{\theta}_1{}^2+F_2\dot{\theta}_4{}^2+G_2\dot{\theta}_1\dot{\theta}_4\right) \quad (14)$$

Where,

$$A_1 = 2\,(W_1 + W_4) + 2\,(W_3 + W_5)\,Z_1{}^2 + 2\,W_6\,Z_1\,Z_5 + 2\,Z_3{}^2\,(W_7 + W_9)$$

$$B_1 = 2\,Z_1\,Z_2\,(W_3 + W_5) + (W_6 + Z_2 + Z_5) + 2\,Z_3\,Z_4\,(W_7 + W_9) + (W_{10} + Z_3 + Z_6 + Z_3 + Z_6)$$

$$C_1 = 4\,(W_3 + W_5)\,Z_1\frac{dZ_1}{dt} + 2\,W_6\,Z_1\,\frac{dZ_5}{dt} + 2\,W_6\,Z_5\,\frac{dZ_1}{dt} + 4\,(W_7 + W_9)\,Z_3\,\frac{dZ_3}{dt}$$

$$D_1 = 2\,(W_3 + W_5)\,Z_1\,\frac{dZ_2}{dt} + 2\,(W_3 + W_5)Z_2\,\frac{dZ_1}{dt} + W_6\,Z_2\,\frac{dZ_5}{dt} + W_6\,Z_5\,\frac{dZ_2}{dt} + 2\,(W_7 + W_9)Z_3\,\frac{dZ_4}{dt} + W_{10}\,Z_6\,\frac{dZ_3}{dt}$$

$$E_1 = 2\,(W_3 + W_5)\,Z_1\frac{dZ_1}{d\theta_1} + 2\,(W_7 + W_9)Z_3\,\frac{dZ_3}{d\theta_1} + W_6\,Z_1\,\frac{dZ_5}{d\theta_1} + W_6\,Z_5\,\frac{dZ_1}{d\theta_1}$$

$$F_1 = 2\,(W_3 + W_5)\,Z_2\frac{dZ_2}{d\theta_1} + 2\,(W_7 + W_9)Z_4\,\frac{dZ_4}{d\theta_1} + W_{10}\,Z_4\,\frac{dZ_6}{d\theta_1} + W_{10}\,Z_6\,\frac{dZ_4}{d\theta_1}$$

$$G_1 = 2\,(W_3 + W_5)\,Z_1\frac{dZ_2}{d\theta_1} + 2\,(W_3 + W_5)Z_2\,\frac{dZ_1}{d\theta_1} + W_6\,Z_2\,\frac{dZ_5}{d\theta_1} + W_6\,Z_5\,\frac{dZ_2}{d\theta_1} + 2\,(W_7 + W_9)\,Z_3\,\frac{dZ_4}{d\theta_1} + 2\,(W_7 + W_9)\,Z_4\,\frac{dZ_3}{d\theta_1} + W_{10}\,Z_3\,\frac{dZ_6}{d\theta_1} + W_{10}\,Z_6\,\frac{dZ_3}{d\theta_1}$$

$$A_2 = 2\,(W_3 + W_5)\,Z_1\,Z_2 + W_6\,Z_2Z_5 + 2\,(W_7 + W_9)Z_3Z_4 + W_{10}\,Z_3\,Z_6$$

$$B_2 = 2\,(W_2 + W_8) + 2\,(W_3 + W_5)\,Z_2{}^2 + 2\,(W_7 + W_9)\,Z_4{}^2 + (W_{10} + Z_4 + Z_6)$$

$$C_2 = 2\,(W_3 + W_5)\,Z_1\frac{dZ_2}{dt} + 2\,(W_3 + W_5)Z_2\,\frac{dZ_1}{dt} + W_6\,Z_2\,\frac{dZ_5}{dt} + W_6\,Z_5\,\frac{dZ_2}{dt} + 2\,(W_7 + W_9)Z_3\,\frac{dZ_4}{dt} + 2\,(W_7 + W_9)Z_4\,\frac{dZ_3}{dt} + W_{10}\,Z_3\,\frac{dZ_6}{dt} + W_{10}\,Z_{10}\,\frac{dZ_3}{dt}$$

$$D_2 = 4\,(W_3 + W_5)\,Z_2\frac{dZ_2}{dt} + 4\,(W_7 + W_9)Z_4\frac{dZ_4}{dt} + 2W_{10}\,Z_4\frac{dZ_6}{dt} + 2\,W_{10}\,Z_6\frac{dZ_4}{dt}$$

$$E_2 = 2\,(W_3 + W_5)\,Z_1\frac{dZ_1}{d\theta_4} + W_6\,Z_1\frac{dZ_5}{d\theta_4} + W_6\,Z_5\frac{dZ_1}{d\theta_4} + 2\,(W_7 + W_9)\,Z_3\frac{dZ_3}{d\theta_4}$$

$$F_2 = 2\,(W_3 + W_5)\,Z_2\frac{dZ_2}{d\theta_4} + 2\,(W_7 + W_9)\,Z_4\frac{dZ_4}{d\theta_4} + W_{10}\,Z_4\frac{dZ_6}{d\theta_4} + W_{10}\,Z_6\frac{dZ_4}{d\theta_4}$$

$$G_2 = 2\,(W_3 + W_5)\,Z_1\frac{dZ_2}{d\theta_4} + 2\,(W_3 + W_5)\,Z_2\frac{dZ_1}{d\theta_4} + W_6\,Z_2\frac{dZ_5}{d\theta_4} + W_6\,Z_5\frac{dZ_5}{d\theta_4} + 2\,(W_7 + W_9)\,Z_3\frac{dZ_4}{d\theta_4} + W_{10}\,Z_6\frac{dZ_3}{d\theta_4} + 2\,(W_7 + W_9)\,Z_4\frac{dZ_3}{d\theta_4} + W_{10}\,Z_3\frac{dZ_6}{d\theta_4}$$

Where,

$$W_1 = \frac{1}{6}\,m_A\,{L_1}^2 \qquad W_2 = \frac{1}{6}\,m_D\,{L_4}^2$$

$$W_3 = \frac{1}{24}\,m_B\,{L_2}^2 \qquad W_4 = \frac{1}{2}\,m_B\,{L_1}^2$$

$$W_5 = \frac{1}{8}\,m_B\,{L_2}^2 \qquad W_6 = \frac{1}{2}\,m_B\,L_1\,L_2$$

$$W_7 = \frac{1}{24}\,m_C\,{L_3}^2 \qquad W_8 = \frac{1}{2}\,m_C\,{L_4}^2$$

$$W_9 = \frac{1}{8}\,m_C\,{L_3}^2 \qquad W_{10} = \frac{1}{4}\,m_C\,L_3\,L_4$$

$$Z_1 = \frac{\partial\,\theta_2}{\partial\,\theta_1} = \frac{L_1\,\sin(\theta_3 - \theta_1)}{L_2\,\sin(\theta_2 - \theta_3)} \qquad Z_2 = \frac{\partial\,\theta_2}{\partial\,\theta_4} = \frac{L_4\,\sin(\theta_4 - \theta_3)}{L_2\,\sin(\theta_2 - \theta_3)}$$

$$Z_3 = \frac{\partial\,\theta_3}{\partial\,\theta_1} = \frac{L_1\,\sin(\theta_2 - \theta_1)}{L_3\,\sin(\theta_2 - \theta_3)} \qquad Z_4 = \frac{\partial\,\theta_3}{\partial\,\theta_4} = \frac{L_4\,\sin(\theta_4 - \theta_2)}{L_3\,\sin(\theta_2 - \theta_3)}$$

$$Z_5 = \cos(\theta_1 - \theta_2) \qquad Z_6 = \cos(\theta_3 - \theta_4)$$

3 Control Techniques

3.1 Nonlinear PID Control

Despite linear fixed parameters PID controllers are often suitable for controlling a simple physical process, the demands for high-performance control with different operating point conditions or environmental parameters are often beyond the abilities of simple PID controllers [12], [19]. The performance of linear PID controllers can be enhanced using several techniques which will be developed to deal with sudden disturbances and complex systems, for example, the PID self-tuning methods, neural networks, and fuzzy logic strategies, and other methods [20], [21].

Among these techniques, nonlinear PID (NLPID) control is presented as one of the most appropriate and effective methods for industrial applications. The nonlinear PID (NLPID) control is carried out in two broad categories of applications. The first category is particular to nonlinear systems, where NLPID control is used to absorb the nonlinearity. The second category deals with linear systems, where NLPID control is used to obtain enhanced performance not realizable by a linear PID control, such as reduced over-shoot, diminished rise time for the step or rapid command input, obtained better-tracking accuracy, and used to compensate the nonlinearity and disturbances in the system [22]. The NLPID controllers have the advantage of high initial gain to achieve fast dynamic response, followed by a low gain to avoid unstable behavior. In this study, the traditional linear PID controller can be enhanced by combining a sector-bounded nonlinear gain into linear fixed gain PID control architecture.

The proposed enhanced nonlinear PID (NLPID) controller consists of two parts. The first part is a sec-tor bounded nonlinear gain $K_n(e)$ while the second part is a linear fixed-gain PID controller (K_p, K_i and K_d). The nonlinear gain $K_n(e)$ is a sector-bounded function of the

error $e(t)$. The previous researches have been considered the nonlinear gain $K_n(e)$ as a one scalar value.

The new in this research, the one scalar value of $K_n(e)$ will be replaced with a row vector that can be expressed as $K_n(e) = [K_{n1}(e) \;\; K_{n2}(e) \;\; K_{n3}(e)]$ as shown in Fig. 5 which will lead to improving the performance of nonlinear PID controller where the values of nonlinear gains will be adjusted according to the error and the type of fixed parameters (K_p, K_i and K_d).

The proposed form of NLPID control can be described as follows.

$$u(t)=K_p[K_{n1}(e).\, e(t)]+K_i\int_0^t [K_{n2}(e).\, e(t)]\, dt + K_d\left[K_{n3}(e).\, \frac{de(t)}{dt}\right] \quad (15)$$

Where $K_{n1}(e), K_{n2}(e)\ and\ K_{n3}(e)$ are nonlinear gains. The nonlinear gains represent any general nonlinear function of the error which is bounded in the sector $0 < K_n(e) < K_n(e)\max$.

There is a wide range of choices available for the nonlinear gain $K_n(e)$. One simple form of the nonlinear gain function can be described as.

$$K_{ni}(e) = ch(w_i e) = \frac{\exp(w_i e) + \exp(-w_i e)}{2} \quad (16)$$

Where $i = 1, 2, 3.$

$$e = \begin{cases} e & |e| \le e_{max} \\ e_{max}\,sgn(e) & |e| > e_{max} \end{cases} \quad (17)$$

The nonlinear gain $K_n(e)$ is lower bounded by $K_n(e)\min = 1$ when $e = 0$, and upper-bounded by $K_n(e)\max = ch(w_i\, e_{max})$. Therefore, e_{max} stand for the range of deviation, and w_i describes the rate of variation of $K_n(e)$.

The critical point in the PID and NLPID controllers is selecting the proper parameters to be appropriate for the controlled plant.

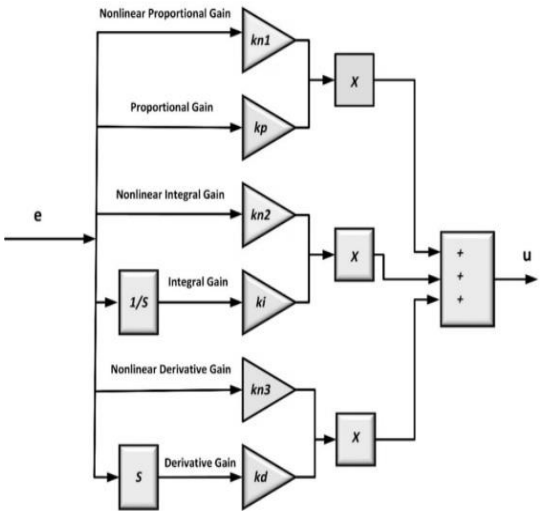

Fig. 5. The enhanced Nonlinear PID Controller structure.

There are different approaches to find the parameters of PID controller, for instance, try and error and Ziegler-Nichols method but, most of these approaches are rough roads. In this paper, the flower pollination optimization technique will be used to obtain the optimal values of both PID and NLPID controllers.

3.2 The Flower Pollination (FP)

In nature, the objective of flower pollination (FP) is the survival of the fittest and optimal reproduction of flowering plants. Pollination in flowering plants can take two major forms, i.e. biotic and abiotic [11]. About 90% of flowering plants belong to biotic pollination. Pollen is transferred by a pollinator such as bees, birds, insects, and animals about 10% remaining of pollination take abiotic such as wind and diffusion in water. Pollination can be achieved by self-pollination or cross-pollination. Self-pollination is the fertilization of one flower from the pollen of the same flower (Autogamy) or different flowers of the same plant (Geitonogamy).

They occur when the flower contains both male and female gametes. Self-pollination usually occurs at a short distance without pollinators. It is regarded as local pollination. Cross-pollination, Allogamy, occurs when pollen grains are moved to a flower from another plant.

The process happens with the help of biotic or abiotic agents as pollinators. Biotic, cross-pollination may occur at a long distance with biotic pollinators. It is regarded as global pollination. Bees and birds as biotic pollinators behave Lévy flight behavior [23] with jump or fly distance steps obeying a Lévy distribution. The FPA algorithm was proposed by Yang [24].

The FP optimization has been used to determine the optimal values for the six parameters that are important in the design of the NLPID control, these parameters are $K_p, K_i,\ K_d, w_1, w_2$ and w_3. The used objective function for this purpose is as follows equation (17).

$$f = \frac{1}{(1-e^{-\beta})(M_p+e_{ss})+e^{-\beta}(t_s-t_r)} \quad (18)$$

The actual closed-loop specification of the system with controller, rise time (t_r), maximum overshoot (M_p), settling time (t_s), and steady-state error (e_{ss}).

This objective function can fulfill the designer's requirement using the weighting factor value (β). The factor is set larger than 0.7 to reduce overshoot and steady-state error. If this factor is set smaller than 0.7 the rise time and settling time will be reducing [25]. Comparison between Nonlinear PID Controller and PID Controller by using flower pollination algorithm to optimize the performance of variables as shown in the Table 1 below:

Table. 1. Parameters Value

PID	NLPID
Kp = 20	Kp = 90
Ki = 3	Ki = 3.5
Kd = 5	Kd = 1.3
-	W1 = 0.19
-	W2 = 3
-	W3 = 1.14

3.3 The Model Reference Adaptive Control (MRAC)

An adaptive controller consists of two loops, an outer loop or normal feedback loop and an inner loop or parameter adjustment loop as shown in Fig. 6.

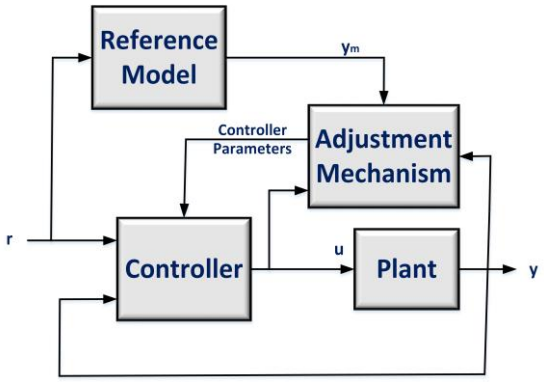

Fig. 6. The model reference adaptive control system.

The MIT rule is the original approach to model-reference adaptive control. The name is derived from the fact that it was developed at the Instrumentation Laboratory (now the Draper Laboratory) at MIT. To adjust parameters in such a way that the loss function is minimized [15-16].

$$J(\theta) = \frac{1}{2}e^2 \tag{19}$$

To make J small, it is reasonable to change the parameters in the direction of the negative gradient of J, that is,

$$\frac{d\theta}{dt} = -\gamma \frac{\partial J}{\partial \theta} = -\gamma e \frac{\partial e}{\partial \theta} \tag{20}$$

Where:

γ: Adaptation rate.
e: The error between the output speed of the motor and the model reference output.
θ: The controller parameter.
From Fig. 10 assume the motor is described by the single-input, single-output (SISO) system.

$$A.y(t) = B\big(u(t) + v(t)\big) \tag{21}$$

Where:
A & B are polynomials depend on the DC motor.
$u(t)$: The output of controller.
$y(t)$: The output speed of motor.
$v(t)$: The process disturbance.
The controller is described in (7).

$$R.u(t) = T.u_c(t) - S.y(t) \tag{22}$$

Where:
R, T and S are controller polynomials.
$u_c(t)$: The desired speed of motor.
Substituting (22) into (21) will result (23)

$$y(t) = \frac{BT}{AR+BS}\, u_c(t) + \frac{BR}{AR+BS}\, v(t) \tag{23}$$

The reference model is described by the single-input, single-output (SISO) system as follow.

$$A_m.y_m(t) = B_m.u_c(t) \Longrightarrow y_m(t) = \frac{B_m}{A_m}\, u_c(t) \tag{24}$$

Where:
A_m, B_m are polynomials depend on the reference model.
$y_m(t)$: The output of model reference.
Assuming $v(t) = 0$ therefore:

$$y(t) = y_m(t) \quad \Longrightarrow \quad \frac{BT}{AR+BS} = \frac{B_m}{A_m} \tag{25}$$

Let the transfer function of reference model is

$$\frac{y_m}{u_c} = \frac{b_m}{a_{m1}P^2 + a_{m2}P + a_{m3}} \tag{26}$$

Where:

$P = \dfrac{d}{dt}$

$a_{m1}, a_{m2}, a_{m3}, b_m$: The model reference transfer function coefficient.
Assume the transfer function of the motor is

$$\frac{y}{u} = \frac{b}{a_1P^2 + a_2P + a_3} \tag{27}$$

a_1, a_2, a_3, b: motor transfer function coefficient.
The diophantine equation is $AR + BS = A_0A_m$ (28)
Where:
A=$a_1P^2 + a_2P + a_3$, $A_m = a_{m1}P^2 + a_{m2}P + a_{m3}$ and A_0 is a gain.
R and S are controller polynomials.

$$\deg(S) = \deg(A) - 1 = 2 - 1 = 1$$
$$\Longrightarrow S = s_0 + Ps_1 \tag{29}$$

Where deg is the polynomial degree.

$$\deg(R) = \deg(S) \quad \Longrightarrow \quad R = r_0 + r_1P \tag{30}$$
$$\deg(A_0) = \deg(A) + \deg(R) - \deg(A_m)$$
$$= 2 + 1 - 2 = 1$$
$$A_o = \tag{31}$$
Similarly $T = P$ (32)

Substituting equations (29, 30, 31 and 32) into equation (21) will result (33)

$$(r_0 + r_1P)u = P.u_c - (s_1P + s_0)y \tag{33}$$
$$u = \frac{P}{R(P)}u_c - \frac{S(P)}{R(P)}y \tag{34}$$

From equation (6) and assume $v(t) = 0$

$$(a_1P^2 + a_2P + a_3) = bu \tag{35}$$

Substituting (34) into (35) will result (36)

$$(a_1P^2 + a_2P + a_3)y = b\left(\frac{T(P)}{R(P)}u_c - \frac{S(P)}{R(P)}y\right) \quad (36)$$

$$\Longrightarrow \quad \left((a_1P^2 + a_2P + a_3) + b\frac{S(P)}{R(P)}\right) = b\frac{T(P)}{R(P)}u_c$$

Equation (21) may be written as follow

$$y = \frac{bT(P)}{(a_1P^2+a_2P+a_3)R(P)+b.S(P)}u_c \quad (37)$$

$$e = y - y_m \quad (38)$$

Substituting equation (11, 22) into (23)

$$e = \left(\frac{bT(P)}{(a_1P^2+a_2P+a_3)R(P)+bS(P)} - \frac{b_m}{a_{m1}P^2+a_{m2}P+a_{m3}}\right)u_c \quad (39)$$

$$\frac{\partial e}{\partial T} = \frac{b}{(a_1P^2+a_2P+a_3)R(P)+bS(P)}u_c \quad (40)$$

$$\frac{\partial e}{\partial S} = \frac{-b^2T(P)}{\left((a_1P^2+a_2P+a_3)R(P)+bS(P)\right)^2}u_c \quad (41)$$

From equation (5)

$$\frac{\partial T}{\partial t} = -\gamma e\frac{b}{(a_1P^2+a_2P+a_3)R(P)+bS(P)}u_c$$

$$\frac{\partial T}{\partial t} = -\gamma' e\frac{1}{(a_1P^2+a_2P+a_3)R(P)+bS(P)}u_c \quad (42)$$

Where

$$\gamma' = b\gamma \quad (43)$$

Similarly $$\frac{\partial S}{\partial t} = -\gamma' e\frac{1}{a_{m1}P^2+a_{m2}P+a_{m3}}y \quad (44)$$

$$\frac{B_m}{A_m} = \frac{\omega_n^2}{p^2+2\xi\omega_n p+\omega_n^2} \quad (45)$$

Where:

$\xi\ (damping\ ratio) = 1.$

$\omega_n\ (natural\ frequency) = 1000.$

(Selected by designer)

MRAC is designed to eliminate the difference between the output of reference model and the actual speed. It does not take into account the error between reference speed and actual speed. This will cause high overshooting and high settling time. This disadvantage can be alleviated by adopting PID compensator as displayed in Fig. 7.

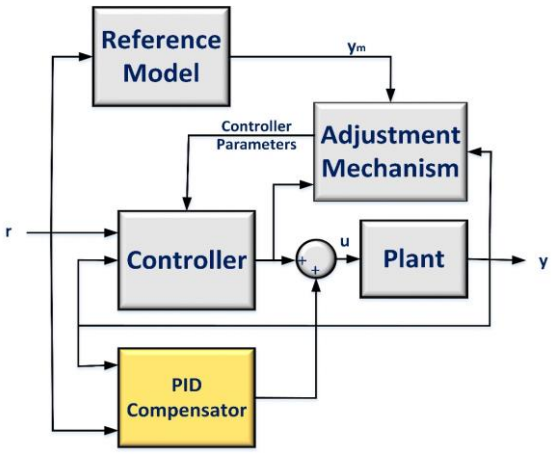

Fig. 7. Block diagram of MRAC with PID compensator.

4 Simulation Results

This section shows a comparative study for the proposed control techniques applied on the pantograph mechanism.

Fig. 8 shows the dynamic response of θ1 for each control technique applied to the pantograph model. It can be noted the MRAC with PID compensator has a faster response compared to the FP-based PID and NLPID controllers. Also, the FP-based PID controllers suffer from high steady-state error. Moreover, the MRAC with PID compensator has a very small overshoot while it has a relatively high undershoot.

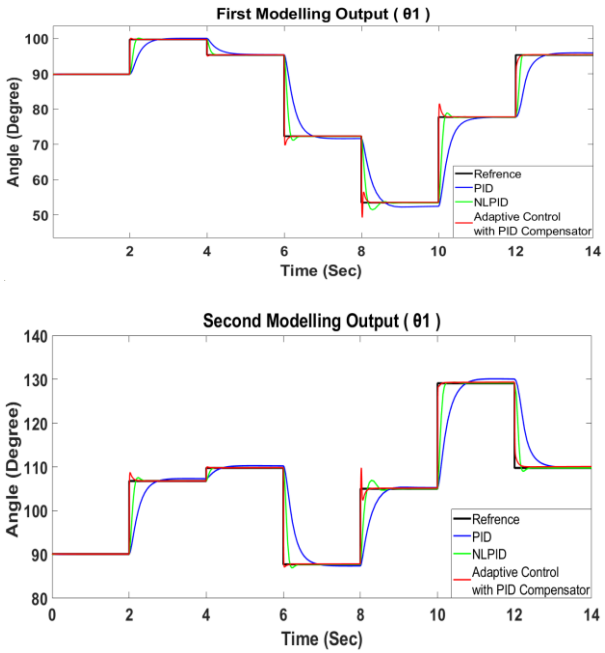

Fig. 8. The position response of θ1 and θ4 through the control techniques.

Fig. 9 demonstrates the corresponding velocity responses of θ1 and θ4 for control techniques. It is obvious that the MRAC with PID compensator has a high-velocity response compared to the FP-based PID and NLPID controllers. Also, the velocity peak of the FP-based PID controller is very low in contrast to the MRAC with PID compensator.

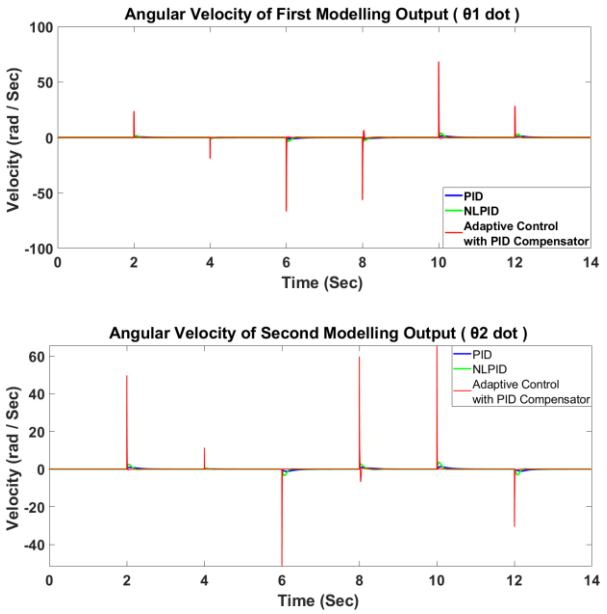

Fig. 9. The velocity of both modeling output: velocity of θ1 and θ4 both as m/s.

Fig. 10 illustrates the corresponding output torque of controllers. It is clear that the MRAC with PID compensator generates a high torque compared to the FP-based PID and NLPID controllers. Also, the torque peak of the FP-based PID controller is very small while the MRAC with PID compensator has high torque in a small period.

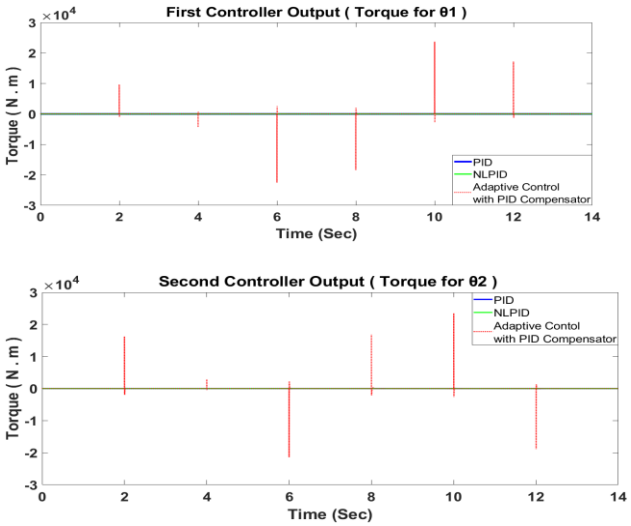

Fig. 10. The controller output (torque) is shown for the first controller and the second one respectively.

5 Conclusions

This paper presents a new mathematical model for a closed chain pantograph mechanism, where the boundary conditions are considered. An overall MATLAB Simulink has been implemented to describe the dynamic behavior of the pantograph robot mechanism. The proposed mathematical model for the pantograph and the corresponding model mechanism using the Simscape were validated to give the same results. Moreover, two control techniques were designed. The first control presents the PID controller which had adjusted by Flower Pollination (FP) optimization. The second control is Nonlinear PID (NLPID) controller where its parameters were determined by Flower Pollination (FP) optimization based on a certain objective function. Moreover, an efficient model reference adaptive control was implemented and applied on pantograph mechanism. A rectangle trajectory position reference is applied to the end effector of the pantograph robot. This purpose was done by the proposed controllers to ensure robustness and performance. The simulation results offer that the MRAC with PID compensator gives more accuracy and better performance compared to the PID and NLPID controllers. The end effector has a less rise time and settling time with high accuracy and low vibration at the MRAC with PID compensator.

6 Acknowledgments

The authors would like to offer thanks to Dr. Mohamed Abdel-Ghany, Faculty of Engineering, 6th October University, for his great efforts in this paper

References:

[1] B. Zi, J. Cao, and Z. Zhu, "Dynamic simulation of hybrid-driven planar five-bar parallel mechanism based on simmechanics and tracking control," Int. J. Adv. Robot. Syst., vol. 8, no. 4, pp. 28–33, 2011, doi: 10.5772/45683.

[2] I. Chavdarov, "Kinematics and Force Analysis of a five-link mechanism by the four spaces Jacoby Matrix," Probl. Eng. Cybern. Robot. 55, vol. 55, pp. 53–63, 2005.

[3] S. Jian and L. Rolland, "Imece2014-37602 Five Bar Planar Manipulator Simulation and Analysis By Bond," in Proceedings of the ASME 2014 International Mechanical

Engineering Congress and Exposition, 2014, pp. 1–7.

[4] R. Hosseinzadeh and M. Zarebnia, "Application and comparison of the two efficient algorithms to solve the pantograph Volterra fuzzy integro-differential equation," Soft Comput., vol. 25, no. 10, pp. 6851–6863, 2021, doi: 10.1007/s00500-021-05691-8.

[5] S. Kosari, Z. Shao, M. Yadollahzadeh, and Y. Rao, "Existence and Uniqueness of Solution for Quantum Fractional Pantograph Equations," Iran. J. Sci. Technol. Trans. A Sci., vol. 1, 2021, doi: 10.1007/s40995-021-01124-1.

[6] J. W. Yoon, J. Ryu, and Y. K. Hwang, "Optimum design of 6-DOF parallel manipulator with translational/rotational workspaces for haptic device application," J. Mech. Sci. Technol., vol. 24, no. 5, pp. 1151–1162, 2010, doi: 10.1007/s12206-010-0321-8.

[7] C. M. Pappalardo, M. C. De Simone, and D. Guida, "Multibody modeling and nonlinear control of the pantograph/catenary system," Arch. Appl. Mech., vol. 89, no. 8, pp. 1589–1626, 2019, doi: 10.1007/s00419-019-01530-3.

[8] G. Campion, Q. Wang, and V. Hayward, "The pantograph Mk-II: A haptic instrument," 2005 IEEE/RSJ Int. Conf. Intell. Robot. Syst. IROS, pp. 723–728, 2005, doi: 10.1109/IROS.2005.1545066.

[9] J. Pilecki, M. A. Bednarczyk, and W. Jamroga, "Model checking properties of multi-agent systems with imperfect information and imperfect recal"l, vol. 322. 2014.

[10] M. A. Rushdi, A. A. Hussein, T. N. Dief, S. Yoshida, and R. Schmehl, "Simulation of the transition phase for an optimally-controlled tethered vtol rigid aircraft for airborne wind energy generation," AIAA Scitech 2020 Forum, vol. 1 PartF, no. January, pp. 1–12, 2020, doi: 10.2514/6.2020-1243.

[11] R. S. Umamaheswara Raju, V. V. S. S. S. Chakravarthy, and P. S. R. Chowdary, "Flower pollination algorithm based reverse mapping methodology to ascertain operating parameters for desired surface roughness," Evol. Intell., vol. 14, no. 2, pp. 1145–1150, 2021, doi: 10.1007/s12065-021-00574-1.

[12] Y. X. Su, D. Sun, and B. Y. Duan, "Design of an enhanced nonlinear PID controller," Mechatronics, vol. 15, pp. 1005–1024, 2005, doi: 10.1016/j.mechatronics.2005.03.003.

[13] Z. Sabir, M. A. Z. Raja, D.-N. Le, and A. A. Aly, "A neuro-swarming intelligent heuristic for second-order nonlinear Lane–Emden multi-pantograph delay differential system," Complex Intell. Syst., no. 0123456789, 2021, doi: 10.1007/s40747-021-00389-8.

[14] S. Łukasik, "Study of Flower Pollination Algorithm for Continuous Optimization," Adv. Intell. Syst. Comput., vol. 322, pp. 451–459, 2014.

[15] A. A. El-samahy and M. A. Shamseldin, "Brushless DC motor tracking control using self-tuning fuzzy PID control and model reference adaptive control," Ain Shams Eng. J., 2016, doi: 10.1016/j.asej.2016.02.004.

[16] M. A. Abdel Ghany and M. A. Shamseldin, "Model reference self-tuning fractional order pid control based on for a power system stabilizer," Int. J. Power Electron. Drive Syst., vol. 11, no. 3, pp. 1333–1434, 2020, doi: 10.11591/ijpeds.v11.i3.pp1333-1343.

[17] L. Abdullah et al., "Evaluation on Tracking Performance of PID, Gain Scheduling and Classical Cascade P / PI Controller on XY Table Ballscrew Drive System Faculty of Manufacturing Engineering, Universiti Teknikal Malaysia Melaka (UteM)," World Appl. Sci. J. 21(Special Issue Eng. Technol., vol. 21, pp. 1–10, 2013, doi: 10.5829/idosi.wasj.2013.21.1001.

[18] T. Nadu and P. Magnet, "Modeling and Implementation of Intelligent Commutation System for BLDC Motor in Underwater Robotic Applications," in 1st IEEE International Conference on Power Electronics. Intelligent Control and Energy Systems (ICPEICES-2016) Modeling, 2016, pp. 1–4.

[19] S. B. U, "Multivariable Centralized Fractional Order PID Controller tuned using Harmony search Algorithm for Two Interacting Conical Tank Process," in SAI Intelligent Systems Conference 2015 November 10-11, 2015 | London, UK Multivariable, 2015, pp. 320–327.

[20] P. Zhao and Y. Shi, "Robust control of the A-axis with friction variation and parameters uncertainty in five-axis CNC machine tools," J. Mech. Eng. Sci., 2014, doi: 10.1177/0954406213519759.

[21] B. B. Reddy, "Modelling and Control of 2-DOF Robotic Manipulator Using BLDC Motor," Int. J. Sci. Eng. Technol. Res. (IJSETR), Vol. 3, Issue 10, Oct. 2014 Model., vol. 3, no. 10, pp. 2760–2763, 2014.

[22] M. A. A. Ghany, M. A. Shamseldin, and A. M. A. Ghany, "A Novel Fuzzy Self Tuning Technique of Single Neuron PID Controller for Brushless DC Motor," Int. J. Power Electron. Drive Syst., vol. 8, no. 4, pp. 1705–1713, 2017, doi: 10.11591/ijpeds.v8i4.pp1705-1713.

[23] A. A. E.-S. Adel A. A. El-Gammal, "Adaptive Tuning of a PID Speed Controller for DC Motor Drives Using Multi-Objective Particle Swarm Optimization MOPSO," 2009.

[24] N. A. Elkhateeb and R. I. Badr, "Novel PID Tracking Controller for 2DOF Robotic Manipulator System Based on Artificial Bee Colony Algorithm," Electr. Control Commun. Eng., vol. 13, no. 1, pp. 55–62, 2017, doi: 10.1515/ecce-2017-0008.

[25] M. A. Shamseldin, M. Sallam, A. M. Bassiuny, and A. M. A. Ghany, "A new model reference self-tuning fractional order PD control for one stage servomechanism system," WSEAS Trans. Syst. Control, vol. 14, pp. 8–18, 2019.

Contribution of Individual Authors to the Creation of a Scientific Article (Ghostwriting Policy)

The author(s) contributed in the present research, at all stages from the formulation of the problem to the final findings and solution.

Sources of Funding for Research Presented in a Scientific Article or Scientific Article Itself

No funding was received for conducting this study.

Conflict of Interest

The author(s) declare no potential conflicts of interest concerning the research, authorship, or publication of this article.